Title
A MCIROSCOPIC-IMPEDANCE MODEL FOR A ROTATING-DISK ELECTRODE

Authors
Hauser, A.K.
Newman, J.

Publication Date
1989-03-01

LBL-26268
Preprint

Lawrence Berkeley Laboratory
UNIVERSITY OF CALIFORNIA

Materials & Chemical Sciences Division

Submitted to Journal of the Electrochemical Society

A Microscopic-Impedance Model for a Rotating-Disk Electrode

A.K. Hauser and J. Newman

March 1989

Prepared for the U.S. Department of Energy under Contract Number DE-AC03-76SF00098.

DISCLAIMER

LBL-26268

A Microscopic-Impedance Model for a Rotating-Disk Electrode

Alan K. Hauser and John Newman

Department of Chemical Engineering
University of California

and

Materials and Chemical Sciences Division
Lawrence Berkeley Laboratory
One Cyclotron Road
Berkeley, CA 94720

March 21, 1989

LBL-26268

A Microscopic-Impedance Model for a Rotating-Disk Electrode

Alan K. Hauser and John Newman

Department of Chemical Engineering, University of California, and
Materials and Chemical Sciences Division, Lawrence Berkeley Laboratory,
One Cyclotron Road, Berkeley, CA 94720

Abstract

A mathematical model is presented that can calculate the frequency response of the electrode-electrolyte interface accounting for adsorption/desorption reactions and electron-transfer processes. The working algorithm uses double-layer theory, incorporating potential and concentration dependent charge-transfer reactions, as well as including the solution's ohmic potential drop. Mass transfer to a rotating disk is accounted for using a Nernst stagnant diffusion layer, although emphasis is placed on the analysis of the reactions occurring within the electrical double-charge layer. The microscopic model calculates the potentials and surface excesses of all the electroactive species present in the solution at the interfacial planes, making the algorithm a lumped-parameter model. This approach makes its possible to determine easily the frequency dependence of the interfacial impedance for a general reaction mechanism.

1. Introduction

The concept of using ac-impedance techniques to study electrochemical systems has been known for over a hundred years.[1] However, much interest in this method has arisen in recent years due to the availability of computerized data-acquisition systems

---

. keywords: reaction mechanisms, diffuse layer, rotating disk

allowing experiments to be carried out with ease.[2] With this has come controversy in the interpretation of the measured complex-plane impedance data,[3] and previous theoretical work[4] does not always provide a complete and generalized explanation of such results. The goal of this work is to provide a theoretical framework for characterizing the electrical double layer and the coupled mass-transfer boundary layer next to a rotating disk, where emphasis is placed on the interfacial-reaction processes.

A microscopic model has been developed that can calculate the frequency response of an electrode-electrolyte interface. The algorithm accounts for the potential and concentration-dependent adsorption/desorption reactions and electron-transfer reactions. The working model utilizes classical double-layer theory to describe the diffuse layer and also accounts for the ohmic potential drop and a Nernst-stagnant diffusion layer adjacent to the disk. Before describing our approach, a review of the double-layer literature will be given. This also will include a summary of the work previously done in this laboratory as it relates to the frequency dependence of the electrode impedance.

1.1. Double-Layer Description and Review

At the electrode-electrolyte interface, some species in solution may have a preference for being near the metal, which results in a small region at the interface with a nonzero charge density. The ions can be electrostatically attracted to the surface, or they may be bound by covalent (or specific) forces to the solid itself. Thermal agitation in the solution however tends to make the nonspecifically adsorbed ions wander from the interface. The net effect of these two forces, electrostatic and thermal, must balance the

charge due to an excess or deficiency of electrons in a very thin layer (< 0.01 nm) on the metal surface. This is because the entire electrode-electrolyte interface is electrically neutral, even though charge can accumulate at given planes within the interface. The array of specifically adsorbed charged species and oriented dipoles existing at the interface, along with the ions distributed in the diffuse part of the solution, form a double-charge layer. The remainder of this section will be devoted to reviewing the historical development of the physical models that have been used to analyze and explain the electrical double layer.†

A thermodynamic treatment[5] of the electrode-solution interface provides relationships among potential, surface tension, and the composition of the bulk solution for an ideally polarizable electrode. Analysis of the double layer enables the surface concentrations of various species at the interface to be determined. Additionally, the Lippmann equation can be used with the measured variation of surface tension with potential at constant composition to yield the surface charge.

Although thermodynamics at times can be quite useful, we have resorted to a non-thermodynamic approach because we are interested in the structure and detailed concentration and potential profile characteristics of the double layer. Microscopic models of the diffuse and inner parts of the double layer offer an explanation for the behavior of macroscopically measurable quantities and provide a useful picture of the structure of the interface. Structural concepts of the double layer go back to Helmholtz.[6] Diffuse-layer theory was first suggested by Gouy[7] and Chapman[8]

† Its structure only very loosely resembles two charged layers.

independently.

The diffuse region of the double layer is regarded as part of the electrolytic solution, but the electrolyte is not electrically neutral. The distribution of ions adjacent to the charged surface is calculated using the approach of Debye and Hückel.[9] In general terms, the Gouy-Chapman model of point charges in a structureless dielectric medium is thought of as an effective ion atmosphere adjacent to an ion of variable charge. Specifically, the model incorporates the Poisson equation, relating the potential variation to the charge density of an isotropic medium, in addition to using the classical Boltzmann distribution for relating the ionic concentrations to the potential. The analytic solution to these governing equations yields the desired concentration and potential profiles within the diffuse part of the double layer.

Stern[10] modified the Gouy-Chapman model by suggesting the importance of the finite size of ions next to the electrode. Thus, Stern proposed a plane of closest approach of ions to the electrode surface, now commonly called the outer Helmholtz plane, as the inner limit of the diffuse layer. He also recognized that some ions might be held to the electrode in a rigid monolayer through operation of close-range forces, and thus implied the necessity for considering different distances of closest approach for cations and anions.

Grahame,[11] in his well-known review, developed Stern's model in an important way by bringing out the idea that the specifically adsorbed ions are closer to the electrode surface than the plane of closest approach of nonspecifically adsorbed ions. Grahame called the plane of closest approach of the electrical centers of these ions the inner Helmholtz plane (see figure 1). The plane of closest approach of the nonspecifically

adsorbed ions (*e.g.*, solvated ions) is again called the outer Helmholtz plane. Let us now discuss in more detail what is meant by specific adsorption.

Specific adsorption refers to the nature of the forces that attract species toward the electrode surface, which are not purely coulombic. Bockris[12] defines it as the adsorption at the interface between an electronic and ionic conductor that is in excess or deficit of the amount which would be expected to be present at the interface from simple coulombic considerations. The measured concentration of specifically adsorbed ions is subject to chemical interpretation in terms of adsorption isotherms and the energies of specific adsorption, with either the charge or electrode potential as a correlating variable. Parsons,[13], [14] in a series of fundamental investigations, treated the question of isotherm assignment associated with the calculation of the amount of specifically adsorbed ions. Finally, Delahay[15] discusses potential-dependent adsorption kinetics and how the double layer affects the rates of electrode processes. The microscopic model of the electrode-electrolyte interface that we will develop in section 2 has its origins in this approach.

1.2. Theoretical Impedance Review

Let us now turn our attention to a review of the work previously done in this lab as it relates to the frequency dependence of the interfacial impedance. The solution of the transport equations for the time-dependent part of the impedance, without *a priori* separation of the faradaic and double-layer charging current, had only been obtained for two simple cases,[16], [17] until Appel solved these equations for a rotating-disk electrode (RDE) where forced convection occurs.[18] He calculated the disk impedance, taking into

account the ohmic losses in the bulk solution, the resistance to diffusion valid at high Schmidt numbers, and the appropriate boundary conditions at the surface of the disk.

Before the time-dependent disk impedance may be assessed, the steady distributions of current, potential, and concentrations can be obtained as Pierini, Appel, and Newman[19] did using superposition integrals. Their method consists of solving Laplace's equation in the bulk of the solution in the form of a series expression. Because of the thinness of the diffusion layer, the normal component of the current density at the surface of the disk remains unchanged through the diffusion layer. This assumption allows one to match the current obtained from the solution to the diffusion-layer superposition integral with the electrode-kinetic current using an iterative method. In addition to the factors in the steady problem, the dependence of the double-layer structure on composition and potential must be taken into account when solving for the ac part of the impedance. The computation of the oscillating behavior is a linear problem, in contrast to the steady behavior, but is still quite complex.

Appel[18] emphasized that the charge-transfer rate equation and the double-layer effects enter as boundary conditions for the convective-diffusion equation for each species in solution. Though the double layer has a finite thickness and extends into the diffusion layer, the ratio of the double-layer thickness to the diffusion-layer thickness is of the order of 10^{-5}. The concept of separating the diffusion layer and the double layer has been rigorously justified by Newman,[20] for the case when the equilibrium double layer is perturbed by a steady-state current below the limiting current. Appel also assumed this to be true for the time-dependent part.

A rigorous treatment of the double layer is possible only if the concentrations of all the ionic species just outside the double layer are known. Appel and Newman[21] pointed out that a change in the double-layer capacity is caused by the variations in the potential and the composition variations of the species in the solution, including the supporting electrolyte. The latter variations are caused by the influence of migration on the supporting electrolyte and the condition of electroneutrality outside the double layer. The authors included the effect of the supporting electrolyte in their time-dependent calculations of the convective Warburg problem.

It now should be obvious that the analysis of the impedance of an electrochemical cell requires knowledge of the interplay of many factors. The electrode reactions, diffusion, and double-layer charging are all important and were accounted for by Appel.[18] The results give the local current and overpotential distribution for both the real and imaginary parts over the entire disk. Because of the excessive computer time needed for the complex-calculation procedure, it was carried out only once for a single perturbation frequency.

In the rotating-disk system, the nonuniform ohmic potential drop in the solution leads to an inherently nonuniform current distribution,[22] and this is accentuated under ac conditions.[23] In the latter reference, Newman showed that the nonuniform current distribution of a rotating disk causes the capacitive behavior of the disk to change with frequency. In the same paper, the author showed that the frequency dependence of the apparent capacity will be much smaller for a spherical electrode, tangent to an insulating plane, than for a disk embedded in an infinite, insulating plane, with the counterelectrode at infinity. Nisancioğlu and Newman[24] showed that it is possible, in

principle, to attain a uniform distribution of current on a rotating sphere below the limiting current even in the presence of concentration variations at the surface. The analysis also applies to a hemispherical cap on an insulating plane.[25] Therefore, in order to reduce the "frequency-dispersion" effects of the disk due to the nonuniform current distribution, a rotating hemispherical electrode (RHE) is a preferred geometry, because the local impedance of the RHE is representative of the entire electrode surface.

1.3. Present Analysis Approach

A microscopic model based on fundamental governing equations of the electrode-electrolyte interface is presented here. Instead of treating the double layer as a boundary condition to the mass-transfer problem as Appel[18] did, we shall concentrate on analyzing the double layer, accounting for its finite thickness. A simplified Nernst diffusion layer also is applied. Another difference with Appel's approach is the emphasis of this work on the analysis of the reaction processes that take place within the double layer. Previously, only a simple electrode reaction was considered, and specific adsorption was not accounted for. Here, a detailed reaction mechanism consisting of any number of adsorption/desorption and electron-transfer reactions is accounted for. This generalized approach allows a proposed mechanism to be changed easily to account for experimental observations. Only the species and the number of equations change for different mechanisms; the form of the equations is not altered.

Finally, we desire a simple, yet adequate model so that the impedance of the system may be calculated over a wide frequency range at different electrode potentials, as opposed to Appel's complex model that was used for only a single frequency. The

advantage of such a model is that the frequency dependence of the impedance may be calculated with relatively little computer time, so that impedance measurements may be analyzed.

2. Governing Equations

A one-dimensional model of the electrode-electrolyte interface is shown in figure 1. This schematic represents the metal electrode, the inner and diffuse regions of the double layer, and the diffusion boundary layer. A qualitative description of the historical evolution of this physical model was given in the previous section. Here, we would like to present the salient features illustrated in figure 1, before describing the interface under alternating-current conditions.

As mentioned before, the double layer is a small region (thickness is of the order of 1 nm, depending upon the ionic strength of the solution) at the metal-solution interface, where a large electric field and a nonzero charge density exist. Accumulation of charge q_1 occurs at the inner Helmholtz plane due to specific adsorption of one or more of the ionic species in solution. The distance of closest approach of the specifically adsorbed layer of ions is denoted by $y_1 = d_{M-1}$. The plane of closest approach of the nonspecifically adsorbed ions is located at distance $y_2 = d_{M-1} + d_{1-2}$ from the electrode surface. This outer Helmholtz plane represents the thickness of the inner or compact region of the double layer. Thus, the OHP forms the boundary between the inner and the diffuse layer.

A diffuse charge q_2 exists outside the compact layer as a result of the strong electric field which causes the ions to be distributed according to Boltzmann's law. The Debye length λ characterizes the thickness of the diffuse region, and the distance beyond

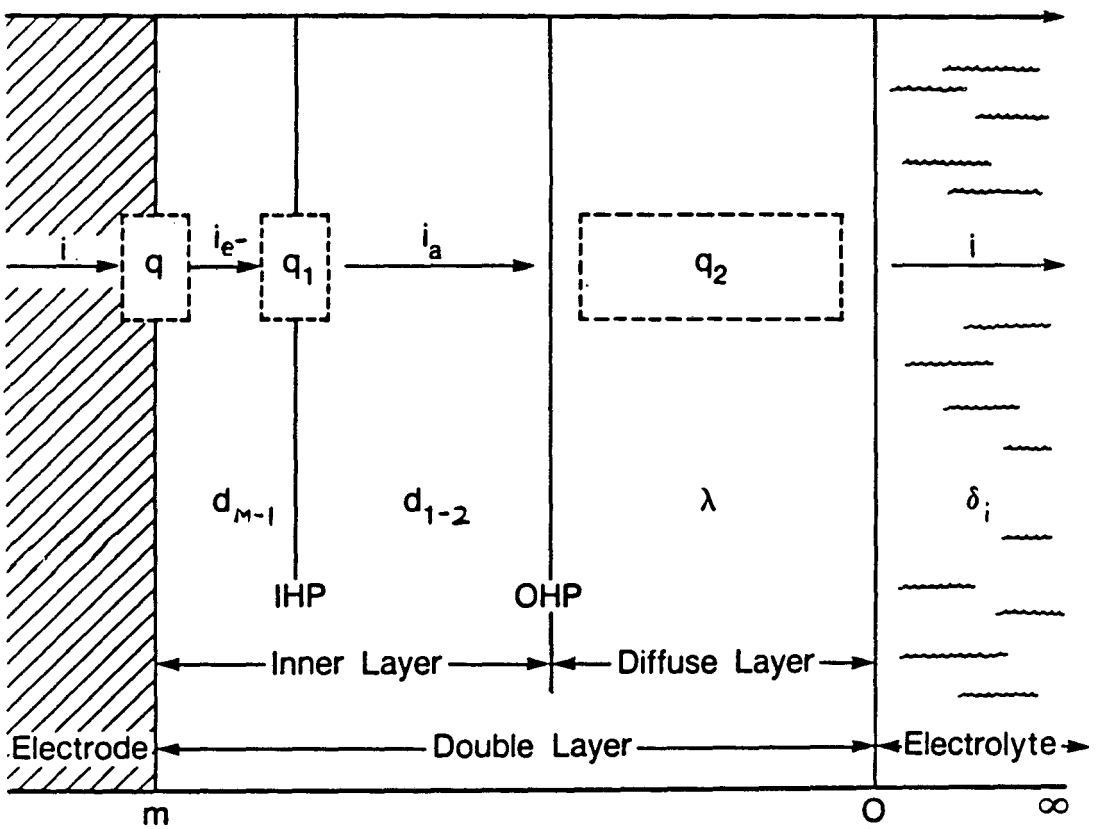

Figure 1. Schematic of the electrode-electrolyte interface illustrating the notation used in the microscopic model.

the diffuse layer to the reference electrode is denoted by δ_i, the diffusion boundary-layer thickness of species i. Finally, the interfacial region as a whole is electrically neutral at steady-state conditions

$$q + q_1 + q_2 = 0 \quad , \tag{1}$$

where q is the charge density on the metal side of the interface, and no large-scale separation of charge can occur. For alternating current, equation 1 will be shown to be generalized later.

Next, we would like to examine the response of the double-layer to an alternating-potential perturbation. The alternating current can pass from the electrode to the solution either by means of faradaic-electrode reactions or by charging the double-layer capacity. Thus, in figure 1 the electronic-conducting current density i is seen to be

$$i = \frac{\partial q}{\partial t} + i_{e^-} \quad , \tag{2}$$

the sum of the charging current density and the electron-transfer-current density i_{e^-}. A charge balance on the inner Helmholtz plane yields the transient current density

$$\frac{\partial q_1}{\partial t} = i_{e^-} - i_a \quad , \tag{3}$$

where i_a is the adsorption current density due to the adsorption/desorption reactions that occur between the IHP and the OHP. Finally, a charge balance on the diffuse layer gives

$$\frac{\partial q_2}{\partial t} = i_a - i \quad , \tag{4}$$

where q_2 is the charge in the diffuse part of the double layer and i is the transient, ionic-conducting current density passed through the electrolyte.

Because of the capacitive effect of the double layer in the presence of an alternating or unsteady current density, it has been customary to represent the impedance of the interface as a capacitor in parallel with a resistor representing the resistance of the charge-transfer process. Even though, it is sometimes possible to use an equivalent circuit to illustrate the system behavior for a specific frequency range for which the circuit is valid, we must note however, the variation of the impedance of an electrochemical system with frequency *cannot* adequately be accounted for by a finite series of resistors, capacitors, and inductors. Therefore, the microscopic model of the interface as shown in figure 1 should prove to be a more fruitful approach for characterizing the impedance of the double layer. Table 1 summarizes the equations and variables found in the microscopic model for n specifically adsorbed species at the inner Helmholtz plane and m species in the diffuse layer and solution. The potential and concentrations are not solved for as continuous functions, but instead are determined only at the interfacial planes, making this a lumped-parameter model.

2.1. Cell Potentials

The first equation in table 1 is for the measurable cell potential, V_{set}, given by $V_{set} = \Phi_m^{\alpha} - \Phi_{RR}^{\alpha'}$, where Φ_m^{α} is the potential of the working metal electrode and $\Phi_{RR}^{\alpha'}$ is the potential of a real reference electrode (*e.g.*, a saturated calomel electrode, SCE) placed in the bulk solution. To obtain detailed kinetic information about reaction mechanisms, we must break down V_{set} into theoretical potential differences that affect the individual elementary reactions. The cavity potential, ψ, therefore, is introduced to characterize the electrical state of the interfacial region, where the potential-dependent

Table 1. Summary of governing equations in lumped-parameter, microscopic model.

Variables	*Equations*	*Number*
$\Delta\psi_2$	Cell Potential, V_{set}	1
$\Delta\psi_{M-1}$	Gauss's Law at IHP	1
$\Delta\psi_{1-2}$	Gauss's Law for Diffuse Region	1
$\Delta\psi_{diff}$	Diffusion Potential	1
$\Delta\psi_{IR}$	Ohmic Drop	1
$\Gamma_{i,1}$	Material Balance at IHP	n
$c_{i,2}$	Boltzmann Distribution	m
$\Gamma_{i,d}$	Modified Boltzmann equation	m
$c_{i,0}$	Material Balance at OHP	m
		$n+3m+5$

charge-transfer reactions occur. The cavity (also called Volta or outer) potential represents the electrical state due to long-range interactions and is a preferred definition of local potential relative to a reference electrode state because it has meaning in all phases (even between phases of dissimilar composition).

The measured cell potential is expressed in terms of cavity potentials as $V_{\text{set}} = \psi_{\text{m}}^{\alpha} - \psi_{\text{m}}^{\alpha'}$ because the difference in electrical state of phases α and α' with identical composition, temperature, and pressure is given by the electrical potential

difference (either the quasi-electrostatic potential or the cavity potential) between the two phases. The total cell potential may be rewritten

$$V_{\text{set}} = (\psi^{\alpha}_{\text{m}} - \psi^{\phi}_{IHP}) + (\psi^{\phi}_{IHP} - \psi^{\epsilon}_{OHP}) + (\psi^{\epsilon}_{OHP} - \psi^{\kappa}_{0}) + (\psi^{\kappa}_{0} - \psi^{\delta}_{\text{b}}) + (\psi^{\delta}_{\text{b}} - \psi^{\alpha'}_{\text{m}}) \quad . \tag{5}$$

These microscopic potential differences are discussed in the appendix.

The first potential difference on the right in equation 5, $\Delta\psi_{M-1} = \psi^{\alpha}_{\text{m}} - \psi^{\phi}_{IHP}$, is the kinetic driving force for electron-transfer reactions. The second potential difference, $\Delta\psi_{1-2} = \psi^{\phi}_{IHP} - \psi^{\epsilon}_{OHP}$, is the kinetic driving force for adsorption/desorption reactions. The third potential difference term in equation 5, $\Delta\psi_2 = \psi^{\epsilon}_{OHP} - \psi^{\kappa}_{0}$, is the potential difference across the diffuse region. The distance from the outer limit of the diffuse layer to the placement of the reference electrode in the bulk solution gives rise to a potential difference, $\Delta\psi_{soln} = \psi^{\kappa}_{0} - \psi^{\delta}_{\text{b}}$. This potential difference can be split into two terms: the diffusion potential $\Delta\psi_{\text{diff}}$ and the ohmic potential difference $\Delta\psi_{IR}$. The diffusion potential is given by the following approximate form of the more general expression given in reference [5]

$$\Delta\psi_{diff} = \frac{F}{\kappa_{\infty}} \sum_{k} z_k D_k \left(c_{k,\infty} - c_{k,0}\right) \quad . \tag{6}$$

The ohmic loss, written in terms of the normal current density i_z, is given by

$$\Delta\psi_{IR} = \int_{0}^{b} \frac{i_z}{\kappa} \, \mathrm{d}z \quad , \tag{7}$$

where z is the axial direction away from the electrode and κ is the conductivity. The 0 refers to just outside the diffuse layer, and b denotes the bulk.

In order to express the ohmic drop, $\Delta\psi_{IR} = A \cdot R_{\Omega} \cdot i$, in terms of lumped parameters, it is necessary to specify a geometry because the components of the ohmic

drop, the area A and the ohmic-resistance R_Ω, both depend on the electrode geometry. For a rotating disk, the primary resistance[26] is $1/4\kappa_\infty r_0$, and the area is πr_0^2. Therefore, $(A \cdot R_\Omega)_{disk} = \pi r_0/4\kappa_\infty$, and the ohmic potential drop can be rewritten as

$$\Delta\psi_{IR} = \frac{\pi r_0}{4\kappa_\infty}\left(\frac{\partial q}{\partial t} + i_{e^-}\right) , \tag{8}$$

where the total current density i is given by equation 2 to be the sum of the double-layer charging-current density and the electron-transfer-current density i_{e^-}. In contrast to the disk, the area of a hemispherical electrode is given by $A = 2\pi r_0^2$, and its primary resistance[24] is $R_\Omega = 1/2\pi\kappa_\infty r_0$. Therefore, $(A \cdot R_\Omega)_{hemi} = r_0/\kappa_\infty$.

The last term in equation 5, $\Delta\psi_{ref} = \psi_b^\delta - \psi_m^{\alpha'}$, is a metal-electrolyte cavity potential difference located in the bulk solution. Finally, equation 5 for the total, measurable cell potential can be expressed as

$$V_{set} = \Delta\psi_{M-1} + \Delta\psi_{1-2} + \Delta\psi_2 + \Delta\psi_{diff} + \Delta\psi_{IR} + \Delta\psi_{ref} \quad . \tag{9}$$

2.2. Gauss's Law

To complete our discussion of the potential variables and their corresponding equations found in table 1, Gauss's law must be introduced. From Maxwell's relations,[27] the variation in the electric field is related to the charge distribution in the system by Poisson's equation

$$\nabla\cdot(\epsilon\mathbf{E}) = -\nabla\cdot(\epsilon\,\nabla\Phi) = \rho_e \quad , \tag{10}$$

where ρ_e is the electric charge density per unit volume and the electric field $\mathbf{E}$ is expressed as the negative gradient of the electrostatic potential Φ, a scalar quantity.

At the interface between two phases, the tangential component of the electric field is continuous. The relationship between the normal components of the electric field in the two phases can be obtained by applying equation 10 to a "pill box" enclosing a portion of the interface (see figure 1, where the three charge densities are enclosed by dotted lines). By means of the divergence theorem, equation 10 can be written in terms of integrals over the surface and the volume of an arbitrary region:

$$\oint \epsilon \mathbf{E} \cdot \mathbf{dS} = \int \rho_e \, dV \quad . \tag{11}$$

This is an expression of Gauss's law, which says that the integral of the outward normal component of $\epsilon \mathbf{E}$ over the surface of a closed region is equal to the charge enclosed. Linear potential profiles are assumed in the double layer due to its thinness, and the normal component of the electric field within region j reduces to $E_{nj} = -\Delta\psi_j / d_j$. Application of this result to the inner Helmholtz plane in figure 1 gives the relationship between the potential difference and the charge per unit area at plane 1:

$$\frac{\epsilon_{1-2}}{d_{1-2}} \Delta\psi_{1-2} - \frac{\epsilon_{M-1}}{d_{M-1}} \Delta\psi_{M-1} = q_1 \quad . \tag{12}$$

The charge q_1 accumulates due to specifically adsorbed ions and is related to the surface concentrations of these species at the IHP by

$$q_1 = F \sum_i z_i \Gamma_{i,1} \quad . \tag{13}$$

Next, a similar form of Gauss's law describes the charge build-up q_2 in the diffuse part of the double layer

$$-\frac{\epsilon_{1-2}}{d_{1-2}} \Delta\psi_{1-2} = q_2 = F \sum_i z_i \Gamma_{i,d} \quad . \tag{14}$$

Again, the electric field on the metal side of the space-charge region is related to its respective potential difference, and the electric field at the outer limit of the diffuse

region is negligible. Here, q_2 is related to the surface concentrations of the species in the diffuse layer, $\Gamma_{i,d}$.

A third form of Gauss's law may be written at the metal side of the interface yielding

$$\frac{\epsilon_{M-1}}{d_{M-1}} \Delta\psi_{M-1} = q = -F\Gamma_{e^-} \quad , \tag{15}$$

where q is the surface charge on the metal. The electric field within the metal phase is zero because the potential of the metal electrode is a constant. Equation 15 is not used as independent equation in the model, and therefore is not included in table 1. Let us now turn our attention from the equations for the potential variables to the equations for the surface concentrations.

2.3. Boltzmann Distribution Equations

The definition of the surface excess of an ionic species in the diffuse layer

$$\Gamma_{i,d} = \int_{y_2}^{y_3} (c_i - c_{i,3})\, dy \tag{16}$$

is used with the Boltzmann distribution

$$c_i(y) = c_{i,3} \exp\left(\frac{-z_i F}{RT} \Phi(y)\right) \tag{17}$$

to yield the following expression

$$\Gamma_{i,d} = 2\lambda\, c_{i,0}\left\{ \exp\left(-\frac{z_i F}{2RT} \Delta\psi_2\right) - 1\right\} \quad , \tag{18}$$

where $c_{i,0} = c_{i,3}$. The modified Boltzmann distribution equation 18 is rigorously valid only for the special case where the magnitudes of the ionic charges are all the same.

The Debye length λ characterizes the thickness of the diffuse region and is given by

$$\lambda = \left(\frac{\epsilon RT}{F^2 \sum_i z_i^2 c_{i,0}} \right)^{1/2} . \tag{19}$$

If there are m species present in the diffuse part of the double layer, then there are m equations 18 for the m surface concentrations, $\Gamma_{i,d}$, and m lumped-parameter equations for the concentrations at the OHP, $c_{i,2}$, given by

$$c_{i,2} = c_{i,0} \exp\left(\frac{-z_i F}{RT} \Delta\psi_2 \right) . \tag{20}$$

2.4. Material Balances

The material balances are the remaining equations in table 1 to be discussed. Before presenting these equations for all species at the interface, let us briefly review how the stoichiometry of an electrochemical reaction is accounted for. This accounting procedure is important since we will show that the transient response of the flux of species i is a function of the potential and surface-concentration dependent rates of reaction occurring within the double layer. The general accounting method as outlined here for any charge-transfer reaction accounts for not only electron-transfer reactions but also metal surface reactions (*e.g.*, heterogeneous, nonelectron-transfer alloy reactions) and adsorption/desorption reactions. These reactions may be represented by the general form

$$\sum_i s_{i,l}^{(m)} M_{i(m)}^{z_i} + \sum_i s_{i,l}^{(IHP)} M_{i(ads)}^{z_i} + \sum_i s_{i,l}^{(OHP)} M_{i(soln)}^{z_i} \rightarrow 0 , \tag{21}$$

where every species i in reaction l is represented. The stoichiometric coefficients, the ionic charge number, and the symbol for the chemical formula of the species are given

by $s_{i,l}$, z_i, and M_i, respectively. The first term in equation 21 represents only those species in the solid phase, composed of electrons and metallic atoms, that participate in the metal surface reactions. The second term represents the species at the inner Helmholtz plane, which can participate in the electron-transfer and adsorption/desorption reactions. The third term represents the species at the outer Helmholtz plane and in the bulk solution.

Although equation 21 is general in nature, we need to specify its limitations. Only two types of charge-transfer reactions can be accounted for in the present model of the interface. Species in the first type of reaction, electron-transfer reactions, are represented by the first two terms in equation 21 and must be either in the solid phase or be adsorbed species at the *IHP*. Species at either the *OHP* or in the solution cannot participate the electron-transfer reactions because the rate of these reactions is dependent on the potential difference $\Delta\psi_{M-1}$. The number of electrons n_l transferred in reaction l can be determined based on stoichiometry and the charge number of the species (see equation 26 in table 2). Species in the second type of allowed reaction, adsorption/desorption reactions occurring between the *IHP* and the *OHP*, are represented by the second and third terms in equation 21. The charge Z_l transferred in the adsorption reaction l is given by equation 30 in table 3.

IHP Material Balance

The material balance[5] for a species at the inner Helmholtz plane is

$$\frac{\partial \Gamma_{i,1}}{\partial t} + \nabla_s \cdot \mathbf{J}_{is} = N_i^{(M-1)} - N_i^{(1-2)} \quad , \tag{22}$$

where $\mathbf{J}_{is}$ is the surface flux of species i, $N_i^{(M-1)}$ is the normal component of the flux

between the metal and IHP, and $N_i^{(1-2)}$ is the normal component of the flux evaluated between the IHP and the OHP. For the present one-dimensional model, the radial surface flux J_{is} is zero.

We should now like to express the fluxes $N_i^{(M-1)}$ and $N_i^{(1-2)}$ in terms of the stoichiometry given in equation 21. The flux next to the electrode surface $N_i^{(M-1)}$ is related to the rate r_l of the electron-transfer reaction l, by equation 23 in table 2. The

Table 2. Equations for the model calculation of the flux and the current density associated with the electron-transfer reactions.

Flux:
$$N_i^{(M-1)} = -\sum_l s_{i,l}^{(IHP)} r_{e^-,l} = \sum_l s_{i,l}^{(m)} r_{e^-,l} \tag{23}$$

Electron-transfer-reaction rate expression:

$$\begin{aligned} r_{e^-,l} = \frac{i_{e^-,l}}{n_l F} &= k_{f,l}\, \Gamma_{i,1}^{s_{i,l}^{(IHP)}} \exp\left[(1-\beta_l)\,\frac{n_l F}{RT}\,\Delta\psi_{M-1}\right] \Delta\Gamma^{s_{n,l}} \\ &\quad s_{i,l} > 0 \\ &\quad - k_{b,l} \prod_i \Gamma_{i,1}^{-s_{i,l}^{(IHP)}} \exp\left[-\beta_l\,\frac{n_l F}{RT}\,\Delta\psi_{M-1}\right] \Delta\Gamma^{s_{p,l}} \\ &\quad s_{i,l} < 0 \end{aligned} \tag{24}$$

$$\Delta\Gamma = \Gamma_{\max} - \sum_j \Gamma_{j,1}\ , \qquad s_{p,l} = \left[\sum_i s_{i,l}^{(IHP)}\right]_{s_{i,l}>0}\ , \qquad s_{n,l} = \left[-\sum_i s_{i,l}^{(IHP)}\right]_{s_{i,l}<0}$$

Electron–transfer current density:
$$i_{e^-} = \sum_l i_{e^-,l} = F \sum_i z_i N_i^{(M-1)} \tag{25}$$

Stoichiometric relationship:
$$n_l = -\sum_i s_{i,l}^{(IHP)} z_i = \sum_i s_{i,l}^{(m)} z_i \tag{26}$$

---

adsorption/desorption flux $N_i^{(1-2)}$ between the IHP and the OHP is given by equation 27 in table 3, where r_l is the rate of the adsorption/desorption reaction l, written as a function of the adsorption-current density, $i_{a,l}$, in equation 28. The kinetic expressions used for the rate of the charge-transfer reactions are modified forms of the Butler-Volmer equation. The electron-transfer and adsorption rates of reaction are dependent on the potential $\Delta\psi_{M-1}$ and $\Delta\psi_{1-2}$ (equations 24 and 28), respectively. In both equations for reaction l, forward and back reaction rate constants, k_f and k_b, must be specified. Other input parameters in this expression include the symmetry factor, β_l,

Table 3. Equations for the model calculation of the flux and the current density associated with the adsorption/desorption reactions.

Flux:

$$N_i^{(1-2)} = -\sum_l s_{i,l}^{(OHP)} r_{a,l} = \sum_l s_{i,l}^{(IHP)} r_{a,l} \tag{27}$$

Rate expression:

$$\begin{aligned} r_{a,l} = \frac{i_{a,l}}{Z_l F} &= k_{f,l} \prod_{\substack{i \\ s_{i,l}>0}} \Gamma_{i,1}^{s_{i,l}^{(IHP)}} c_{i,2}^{s_{i,l}^{(OHP)}} \exp\left((1-\beta_l)\frac{Z_l F}{RT}\Delta\psi_{1-2}\right)\Delta\Gamma^{s_{n,l}} \\ &- k_{b,l} \prod_{\substack{i \\ s_{i,l}<0}} \Gamma_{i,1}^{-s_{i,l}^{(IHP)}} c_{i,2}^{-s_{i,l}^{(OHP)}} \exp\left(-\beta_l \frac{Z_l F}{RT}\Delta\psi_{1-2}\right)\Delta\Gamma^{s_{p,l}} \end{aligned} \tag{28}$$

Current density:

$$i_a = \sum_l i_{a,l} = F \sum_i z_i N_i^{(1-2)} \tag{29}$$

Stoichiometric relationship:

$$Z_l = -\sum_i s_{i,l}^{(OHP)} z_i = \sum_i s_{i,l}^{(IHP)} z_i \tag{30}$$

and the maximum number of active sites available at the inner Helmholtz plane Γ_{max}.

Finally, we should like to consolidate our notation by rewriting the material balance equation 22 in terms of the general reaction rate r_l as

$$\frac{\partial \Gamma_{i,1}}{\partial t} = -\sum_l s_{i,l}^{(IHP)} r_l \quad , \tag{31}$$

where a general form for r_l is given by

$$\begin{aligned} r_l = {} & k_{f,l} \prod_{\substack{i \\ s_{i,l} > 0}} \Gamma_{i,1}^{s_{i,l}^{(IHP)}} c_{i,2}^{s_{i,l}^{(OHP)}} \exp\left[(1-\beta_l)\frac{Z_l F}{RT}\Delta\psi_l\right] \Delta\Gamma^{s_{n,l}} \\ & - k_{b,l} \prod_{\substack{i \\ s_{i,l} < 0}} \Gamma_{i,1}^{-s_{i,l}^{(IHP)}} c_{i,2}^{-s_{i,l}^{(OHP)}} \exp\left[-\beta_l \frac{Z_l F}{RT}\Delta\psi_l\right] \Delta\Gamma^{s_{p,l}} \quad . \end{aligned} \tag{32}$$

Additionally, the material-balance equation 22 or 32 can be multiplied by Fz_i and summed over all species i yielding the current density relationship given by equation 2.

OHP Material Balance

One additional equation is needed for each concentration $c_{i,0}$ at the outer limit of the diffuse layer to complete the set of equations presented in table 1. The final material balance equation at the OHP describes the relationship between the stoichiometry of the adsorption/desorption reactions and the mass-transfer in the diffusion layer. The conservation equation for each species in the diffuse part of the double layer is

$$\frac{\partial \Gamma_{i,d}}{\partial t} = N_i^{(1-2)} - N_i(z=0) \quad , \tag{33}$$

where the flux $N_i^{(1-2)}$ is given in table 3 by equation 27 and $N_i(z=0)$ is the flux at the

inner limit of the diffusion layer. The flux is given by

$$N_i = -z_i D_i \frac{F}{RT} c_i \nabla\Phi - D_i \nabla c_i + c_i \mathbf{v} \quad , \tag{34}$$

where the terms on the right are due to migration, diffusion, and convection, respectively. The latter flux couples the microscopic model to the macroscopic mass-transfer boundary-layer problem. For the simplified treatment of mass-transfer effects in this paper, equation 34 reduces to

$$N_i(z=0) = -\frac{D_i}{\overline{\delta}_i}(c_{i,\infty} - c_{i,0}) \quad , \tag{35}$$

where $\overline{\delta}_i$ is the Nernst diffusion layer thickness for a rotating disk given by

$$\overline{\delta}_i = 1.6117 D_i^{1/3} \nu^{1/6} \Omega^{-1/2} \quad . \tag{36}$$

Remaining Material Balance

For completeness, we should like to present the material balance for the metal phase

$$\frac{\partial \Gamma_{i,m}}{\partial t} = N_i^{(m)} - N_i^{(M-1)} = -\sum_l s_{i,l}^{(m)} r_l \quad , \tag{37}$$

where r_l represents both metal-phase reactions and electron-transfer reactions. We are not considering metal phase or alloy reactions in this work; therefore, a more general form than is given by equation 37 will not be given here.

3. Method of Solution

We are interested in calculating the frequency response of the interfacial impedance for a specified reaction mechanism. The set of $n + 3m + 5$ governing equations summarized in table 4 must therefore be solved for the unknown

concentrations and potentials using a numerical procedure. The first step of the calculational procedure is to separate the problem into a dc and ac part by writing each model variable in terms of a steady-state and transient contribution.

Each of the variables ($\Delta\psi_j$, $\Gamma_{i,1}$, $\Gamma_{i,d}$, $c_{i,2}$, $c_{i,0}$) is represented by the following equation[†]

$$\chi = \overline{\chi} + \widetilde{\chi} \exp(j\omega t). \tag{38}$$

The second term on the right side of equation 38 is the time-dependent, small-signal perturbation or fluctuation around the steady-state dc level, $\overline{\chi}$, of the variable. The perturbation frequency ω in rad/s is given by $\omega = 2\pi f$ for which f is in Hz, and $j^2 = -1$. The time-independent phasor $\widetilde{\chi}$ is given by

$$\widetilde{\chi} = |\widetilde{\chi}| \exp(j\phi) \tag{39}$$

and is characterized by the magnitude of the perturbation $|\widetilde{\chi}|$ and phase angle ϕ.

Substitution of an expression of the form of equation 39 for each variable into the governing equations yields a set of steady-state equations and another set of equations for the complex variables. The second set of ac equations is no longer time dependent, but is expressed in the frequency domain *(e.g.,* $j\omega\widetilde{\chi}$ replaces $\partial\chi/\partial t$). Before one can solve for the complex variables, a solution to the nonlinear steady-state problem first must be obtained. Thus, the dc form of the equations given in table 4 is solved using an iterative Newton-Raphson multidimensional procedure. These results are then used in the ac calculational procedure. Before discussing the ac-linearization procedure, let us first review the numerical procedure used for solving the steady-state problem.

[†] Strictly speaking, one takes the real part of such complex expressions:
$\chi = \overline{\chi} + \mathrm{Re}\{\widetilde{\chi} \exp(j\omega t)\}$.

Table 4. Summary of the equations in the microscopic model of the interface.

Variables	*Equations*	*Number*
$\Delta\psi_2$	$V_{set} = \Delta\psi_{M-1} + \Delta\psi_{1-2} + \Delta\psi_2 + \Delta\psi_{diff} + \Delta\psi_{IR} + \Delta\psi_{ref}$	1
$\Delta\psi_{M-1}$	$\frac{\epsilon_1}{d_1}\Delta\psi_{1-2} - \frac{\epsilon_0}{d_0}\Delta\psi_{M-1} = F\sum_k z_k\Gamma_{k,1}$	1
$\Delta\psi_{1-2}$	$-\frac{\epsilon_1}{d_1}\Delta\psi_{1-2} = F\sum_k z_k\Gamma_{k,d}$	1
$\Delta\psi_{diff}$	$\Delta\psi_{diff} = \frac{F}{\kappa_\infty}\sum_k z_k D_k(c_{k,\infty} - c_{k,0})$	1
$\Delta\psi_{IR}$	$\Delta\psi_{IR} = \frac{\pi r_0}{4\kappa_\infty} F\sum_l n_l r_{f,l}$	1
$\Gamma_{i,1}$	$\frac{\partial\Gamma_{i,1}}{\partial t} = -\sum_l s_{i,l}^{(IHP)} r_l$	n
$c_{i,2}$	$c_{i,2} = c_{i,0}\exp\left(-\frac{z_i F}{RT}\Delta\psi_2\right)$	m
$\Gamma_{i,d}$	$\Gamma_{i,d} = 2\lambda c_{i,0}\left\{\exp\left(-\frac{z_i F}{2RT}\Delta\psi_2\right) - 1\right\}$	m
$c_{i,0}$	$\frac{\partial\Gamma_{i,d}}{\partial t} = -\sum_l s_{i,l}^{(OHP)} r_{a,l} + \frac{D_i}{\bar{\delta}_i}(c_{i,\infty} - c_{i,0})$	m
		$5+n+3m$

3.1. Numerical-Solution Technique

A multivariable Newton-Raphson method is used to solve iteratively the set of nonlinear dc equations. Each equation is linearized using a Taylor expansion given by

$$f(x_j) = f(x_j^*) + \sum_j \left[\frac{\partial f}{\partial x_j}\right](x_j - x_j^*) \quad , \tag{40}$$

where x_j represents all the variables that the particular equation is a function of. Note that $f = 0$ for the correct solution. The multidimensional Newton's method[28] requires the equations to be cast into a form of

$$\sum_j B_{ij}\,\Delta x_j \;=\; G_i \quad , \tag{41}$$

where $G_i = f(x_j^*)$ is the error vector, $B_{ij} = -\left[\frac{\partial f}{\partial x_j}\right]_{x_j^*}$ is the coefficient matrix, and $\Delta x_j = x_j - x_j^*$ is a vector containing the difference variables. The derivatives B_{ij} are derived analytically and then prescribed into code. Even though this process can become tedious for detailed reaction mechanisms, the algorithm was developed in a general fashion allowing mechanisms to be easily changed, facilitating the mechanistic study. Initial guesses are made for each variable x_j^* and are iterated upon until the convergence criteria are met. Specifically, Newman's[29] MATINV subroutine is used to decompose, invert the matrix, and solve the set of equations.

3.2. Linearization of AC Problem

The governing equations of the microscopic interfacial model must be split into a set of steady-state and a set of transient equations, as was stated earlier. The resulting ac equations, expressed in the frequency domain, are summarized in table 5. The equations involve the complex variables, the potential and concentration phasors, which

are represented by $\tilde{\chi} = \mathrm{Re}\{\tilde{\chi}\} + j\mathrm{Im}\{\tilde{\chi}\}$. Splitting the complex variables into real and imaginary parts yields twice as many frequency-coupled equations. The same numerical technique to solve the set of nonlinear dc equations is used to solve the set of ac equations as a function of frequency at a given cell potential. However, an iterative procedure is not necessary since a linear-response analysis is applied.

The linearized ac equations found in table 5 follow directly from the nonlinear equations given in table 4 by using a Taylor expansion for each variable in the problem. Linearization of the rate of reaction r_l, given by equation 33, yields

$$\tilde{r}_l = \sum_j \frac{\partial r_l}{\partial \Delta\psi_j} \Delta\tilde{\psi}_j + \sum_j \frac{\partial r_l}{\partial \Gamma_{j,1}} \tilde{\Gamma}_{j,1} + \sum_j \frac{\partial r_l}{\partial c_{j,2}} \tilde{c}_{j,2} \quad . \tag{42}$$

A similar equation is used to linearize the flux expressions given in tables 2 and 3.

The final equation in table 5 is not obtained directly from the corresponding equation in equation 4. Instead, the well-known[30] convective-Warburg impedance function for a rotating disk, $-1/\theta'(0)$, is used with the ac flux $\tilde{N}_i = -D_i\,(\,d\tilde{c}_i/dz)_{z=0}$ to yield

$$\tilde{N}_i(z=0) = \frac{-D_i/\delta_i}{-1/\theta'(0)} \tilde{c}_{i,0} \quad , \tag{43}$$

where the prime denotes differentiation with respect to $\xi = z/\delta_i$. The dimensionless impedance function can be approximated[31] by the relation for a stagnant Nernst layer:

$$\frac{-1}{\theta'_N(0)} = \frac{\tanh\left(\Gamma(4/3)\sqrt{jK}\right)}{\sqrt{jK}} \quad , \tag{44}$$

where the dimensionless perturbation frequency is given by

$$K = \frac{\omega}{\Omega}\left(\frac{9\nu}{a^2 D_R}\right)^{1/3} \quad . \tag{45}$$

Table 5. Summary of the ac equations in the microscopic model of the interface.

Variables	*Equations*	*Number*
$\Delta\tilde{\psi}_2$	$\tilde{V}_{set} = \Delta\tilde{\psi}_{M-1} + \Delta\tilde{\psi}_{1-2} + \Delta\tilde{\psi}_2 + \Delta\tilde{\psi}_{diff} + \Delta\tilde{\psi}_{IR}$	2
$\Delta\tilde{\psi}_{M-1}$	$\frac{\epsilon_{1-2}}{d_{1-2}}\Delta\tilde{\psi}_{1-2} - \frac{\epsilon_{M-1}}{d_{M-1}}\Delta\tilde{\psi}_{M-1} = F\sum_k z_k\tilde{\Gamma}_{k,1}$	2
$\Delta\tilde{\psi}_{1-2}$	$-\frac{\epsilon_{1-2}}{d_{1-2}}\Delta\tilde{\psi}_{1-2} = F\sum_k z_k\tilde{\Gamma}_{k,d}$	2
$\Delta\tilde{\psi}_{diff}$	$\Delta\tilde{\psi}_{diff} = \frac{-F}{\kappa_\infty}\sum_k z_k D_k\tilde{c}_{k,0}$	2
$\Delta\tilde{\psi}_{IR}$	$\Delta\tilde{\psi}_{IR} = \frac{\pi r_0}{4\kappa_\infty}\left[F\sum_l n_l\tilde{r}_{f,l} + j\omega\frac{\epsilon_{M-1}}{d_{M-1}}\Delta\tilde{\psi}_{M-1}\right]$	2
$\tilde{\Gamma}_{i,1}$	$j\omega\tilde{\Gamma}_{i,1} = -\sum_l s_{i,l}^{(IHP)}\tilde{r}_l$	$2n$
$\tilde{c}_{i,2}$	$\tilde{c}_{i,2} = \bar{c}_{i,2}\left(\frac{\tilde{c}_{i,0}}{\bar{c}_{i,0}} - \frac{z_i F}{RT}\Delta\tilde{\psi}_2\right)$	$2m$
$\tilde{\Gamma}_{i,d}$	$\tilde{\Gamma}_{i,d} = \bar{\Gamma}_{i,d}\left(\frac{\tilde{c}_{i,0}}{\bar{c}_{i,0}} - \frac{z_i F}{2RT}\Delta\tilde{\psi}_2\right)$	$2m$
$\tilde{c}_{i,0}$	$j\omega\tilde{\Gamma}_{i,d} = -\sum_l s_{i,l}^{(OHP)}\tilde{r}_{a,l} + \frac{D_i/\delta_i}{\left\{\frac{-1}{\theta'(0)}\right\}}\tilde{c}_{i,0}$	$2m$
		$10+2n+6m$

4. Determination of the Impedance

The impedance Z of the electrochemical system is the ratio of the sinusoidal potential perturbation to the current perturbation response at a steady-state potential. The potential-perturbation phasor is given by $\tilde{V}_{set} = |\tilde{V}_{set}|$ since the phase angle, $\phi = 0$, is measured relative to the potential reference signal, and a potentiostatic mode is being simulated.† The alternating-current response is given by $\tilde{i} = |\tilde{i}| \exp(j\phi)$. Equation 2 for the total ac current and equation 15 may be used yielding

$$\tilde{i} = j\omega \frac{\epsilon_{M-1}}{d_{M-1}} \Delta\tilde{\psi}_{M-1} + \tilde{i}_{e^-} \quad , \tag{46}$$

where $\partial q/\partial t$ has been replaced with $j\omega\tilde{q}$. The ac-electron-transfer current density can be expressed in terms of the linearized reaction rate by $\tilde{i}_{e^-} = \sum_l \tilde{i}_{e^-,l} = F \sum_l n_l \tilde{r}_l$.

The total electrochemical impedance is given by

$$Z = \frac{\tilde{V}_{set}}{\tilde{i}} = |Z| \exp(-j\phi) = \mathrm{Re}\{Z\} + j\,\mathrm{Im}\{Z\} \quad , \tag{47}$$

where the magnitude of the impedance,

$$|Z| = \frac{|\tilde{V}_{set}|}{|\tilde{i}|} = \sqrt{\mathrm{Re}\{Z\}^2 + \mathrm{Im}\{Z\}^2} \tag{48}$$

is expressed in ohm·cm^2. The phase shift between the current and the potential is given by $\phi = \arctan(\mathrm{Im}\{Z\}/\mathrm{Re}\{Z\})$. The impedance can now be obtained by multiplying by the complex conjugate of the current density.

---

† Of course, the impedance calculations are independent of this choice of operating mode.

5. Conclusions

A generalized algorithm based on fundamental governing equations has been presented that calculates the frequency response of the electrode-electrolyte interface. The microscopic model is a one-dimensional physical model of the double layer and accounts for a detailed reaction mechanism consisting of any number of potential and concentration-dependent adsorption/desorption and electron-transfer reactions occurring between the interfacial planes. The working model also utilizes classical double-layer theory to describe the diffuse layer, and a stagnant Nernst diffusion layer is applied to the mass-transfer boundary layer. The emphasis of this paper, however, has been on the mechanistic approach that easily allows a proposed mechanism to be changed to account for experimental observations.

The set of nonlinear DC equations and the coupled linear AC equations governing the metal-solution interface can be solved numerically yielding the complex potential and concentration phasors at the interfacial planes; thus, making this a lumped-parameter impedance model. This simple, yet adequate model is capable of calculating the impedance of an electrochemical system over a wide frequency range at different electrode potentials, so that impedance measurements may be analyzed.

Acknowledgements

This work was supported by the Assistant Secretary for Conservation and Renewable Energy, Office of Energy Storage and Distribution, Energy Storage Division, of the U.S. Department of Energy under Contract No. DE–AC03–76SF00098.

List of Symbols

A	area of electrode, cm^2
$c_{i,2}$	concentration of species i at OHP, mol/cm^3
$c_{i,0}$	concentration of species i at the outer limit of the diffuse layer, mol/cm^3
$c_{i,\infty}$	concentration of species i in the bulk solution, mol/cm^3
C	double-layer capacity, F/cm^2
C_j	capacity of region j, F/cm^2
C_d	capacity of the diffuse layer, F/cm^2
C_{M-2}	capacity of region between the metal and the inner limit of the diffuse layer, F/cm^2
C_{M-1}	capacity of region between the metal and the inner Helmholtz plane, F/cm^2
d_{M-1}	distance between metal surface and the inner Helmholtz plane, cm
d_{1-2}	distance between the inner Helmholtz plane and the outer Helmholtz plane, cm
D_i	diffusion coefficient of species i, cm^2/s
e^-	symbol for the electron
$\mathbf{E}$	electric field, V/cm
E_{nj}	normal component of the electric field at position j, V/cm
f	frequency, Hz
F	Faraday's constant, 96,487 C/equiv

i	total current density, A/cm^2
$i_{a,l}$	current density of adsorption/desorption reaction l, A/cm^2
$i_{e^-,l}$	current density of electron-transfer reaction l, A/cm^2
j	$=\sqrt{-1}$ imaginary number
J_{is}	surface flux of species i, mol/cm^2
k_f, k_b	forward and back rate constants for adsorption/desorption reaction
K	dimensionless frequency
m	number of species in the diffuse layer and electrolytic solution
M_i	symbol for the chemical formula of species i
n	number of species at the inner Helmholtz plane
n_l	number of electrons involved in electrode reaction l
N_i	flux of species i, mol/cm^{2}s
q	surface charge density on the metal side of the double layer, C/cm^2
q_1	surface charge density at the inner Helmholtz plane, C/cm^2
q_2	surface charge density in the diffuse part of the double layer, C/cm^2
r_l	rate of charge-transfer reaction l, mol/cm^2-s
r_0	radius of disk, cm
R	universal gas constant, 8.3143 J/mol-K
R_Ω	primary solution resistance, ohm
$s_{i,l}$	stoichiometric coefficient of species i in electrode reaction l
t	time, s

T	absolute temperature, K
V_{set}	specified total set potential (electrode potential relative to given reference electrode placed in the bulk solution), V
$\lvert \widetilde{V}_{set} \rvert$	magnitude of perturbation potential relative to given reference electrode, V
χ	dummy variable
$\overline{\chi}$	time-averaged part of χ
$\widetilde{\chi}$	complex part of χ
$\lvert \widetilde{\chi} \rvert$	magnitude of perturbation χ
z_i	charge number of species i
Z	complex impedance, ohm
Z_l	the number of charge units in adsorption/desorption reaction

Greek symbols:

β_l	transfer coefficient of reaction l
$\Gamma_{i,1}$	surface concentration of species i at the IHP, mol/cm^2
$\Gamma_{i,d}$	surface concentration of species i in the diffuse layer, mol/cm^2
Γ_{max}	maximum number of active surface sites, mol/cm^2
δ_i	diffusion boundary layer thickness for species i, cm
ϵ	permittivity, F/cm or C/V-cm
ς	zeta potential, V
$\Delta\psi_{M-1}$	potential difference between electrode and inner Helmholtz plane, V
$\Delta\psi_{1-2}$	potential difference between inner and outer Helmholtz planes, V

$\Delta\psi_2$	potential difference across the diffuse layer, V
$\Delta\psi_{IR}$	ohmic potential difference, V
$\Delta\psi_{diff}$	diffusion potential, V
$-1/\theta'(0)$	dimensionless Warburg impedance function
κ_∞	conductivity of the bulk solution, ohm^{-1}-cm^{-1}
λ	Debye length, cm
ν	kinematic viscosity, cm^2/s
ξ	dimensionless axial distance
π	3.141592654
ρ_e	electric charge density per unit volume, C/cm^3
ϕ	phase angle
Φ_m	electric potential of the metal electrode, V
Φ_{RR}	potential of a real reference electrode placed in the bulk solution, V
Φ_{RG}	potential of a hypothetical reference electrode of a given kind, V
ω	perturbation frequency, rad/s
Ω	angular rotation speed of disk, rad/s

subscripts:

m	at the metal electrode surface
0	just outside the diffuse part of the double layer
∞	in the bulk electrolyte, where there are no concentration variations
1	at the inner Helmholtz plane
2	at the outer Helmholtz plane

3	just outside the diffuse part of the double layer
superscripts:	
(M-1)	between metal and IHP
(1-2)	between IHP and OHP
(2)	between OHP and outer limit of diffuse layer
(*IHP*)	at the inner Helmholtz plane
(*OHP*)	at the outer Helmholtz plane
—	time-average part
~	complex part

References

[1]. F. Kohlrausch, "Ueber die elektromotorisch Kraft sehr dunner Gasschichten auf Metalplatten," *Poggendorfs Annalen, 148,* 143-154 (1873).

[2]. C. Gabrielli, *Identification of Electrochemical Processes by Frequency Response Analysis,* Solartron Instrumentation Group (1980).

[3]. Boris D. Cahan and Chia-Tien Chen, "The Nature of the Passive Film on Iron, II. A-C Impedance Studies" *Journal of the Electrochemical Society, 129,* 474-480 (1982).

[4]. J. Ross Macdonald, ed., *Impedance Spectroscopy, Emphasizing Solid Materials and Systems,* New York: John Wiley & Sons, 1987.

[5]. John Newman, *Electrochemical Systems,* Englewood Cliffs, N.J.: Prentice-Hall, Inc., 1973.

[6]. H. L. F. von Helmholtz, *Ann. Physik, (2), 89,* 211 (1853).

[7]. G. Gouy, *J. Phys. 9,* 457 (1910).

[8]. D. L. Chapman, *Philos. Mag. 25* (6), 475 (1913).

[9]. P. Debye and E. Hückel, "Zur Theorie der Elektrolyte," *Physikalische Zeitschrift, 24,* 185-206 (1923).

[10]. O. Stern, *Z. Elektrochem. 30,* 508 (1924).

[11]. David C. Grahame, "The Electrical Double Layer and the Theory of Electrocapillarity," *Chemical Reviews, 41,* 441-501 (1947).

[12]. M. A. Habib and J. O'M. Bockris, "Specific Adsorption of Ions" *Comprehensive Treatise of Electrochemistry,* Volume 1: The Double Layer, Edited by J. O'M. Bockris, Brian E. Conway, and Ernest Yeager, Plenum Press, New York, 1980.

[13]. Roger Parsons, "Equilibrium Properties of Electrified Interphases," Chapter 3 in *Modern Aspects of Electrochemistry, 1,* John O'M Bockris, editor, Academic Press, New York, 1954, 103-179.

[14]. Roger Parsons, "The Structure of the Electrical Double Layer and Its Influence on the Rates of Electrode Reactions," *Advances in Electrochemistry and Electrochemical Engineering, 1,* 1-64 (1961).

[15]. Paul Delahay, *Double Layer and Electrode Kinetics* (New York: Interscience Publishers, 1965)

[16]. Karel Holub, Gino Tessari, and Paul Delahay, "Electrode Impedance without *a Priori* Separation of Double-Layer Charging and Faradaic Process," *Journal of Physical Chemistry, 71,* 2612-2618, (1967).

[17]. Eugene Levart and Daniel Schuhmann, "Migration-Diffusion Coupling and the Concept of Electrochemical Impedance," *Journal of Electroanalytical Chemistry and Interfacial Electrochemistry, 24,* 41-52, (1970).

[18]. Peter Appel, Dissertation, University of California, Berkeley (1976).

[19]. Peter Pierini, Peter Appel, and John Newman, "Current Distribution on a Disk Electrode for Redox Reactions," *Journal of the Electrochemical Society, 123,* 366-369 (1976).

[20]. John Newman, "The Polarized Diffuse Double Layer," *Transactions of the Faraday Society, 61,* 2229-2237, (1965).

[21]. Peter Appel and John Newman, "Radially Dependent Convective Warburg Problem for a Rotating Disk," *Journal of the Electrochemical Society, 124,* 1864-1868, (1977).

[22]. John Newman, "Current Distribution on a Rotating Disk below the Limiting Current," *Journal of the Electrochemical Society, 113,* 1235-1241 (1966).

[23]. John Newman, "Frequency Dispersion in Capacity Measurements at a Disk Electrode," *Journal of the Electrochemical Society, 117,* 198-203 (1970).

[24]. Kemal Nisancioglu and John Newman, " Current Distribution on a Rotating Sphere below the Limiting Current," *Journal of the Electrochemical Society, 121,* 241-246 (1974).

[25]. Der-Tau Chin, "Convective Diffusion on a Rotating Spherical Electrode," *Journal of the Electrochemical Society, 118,* 1434-1438 (1971).

[26]. John Newman, "Resistance for flow of Current to a Disk" *Journal of the Electrochemical Society, 113,* 501-502 (1966).

[27]. James Clerk Maxwell, *A Treatise on Electricity and Magnetism,* Vol. I (Oxford: Clarendon Press, 1892).

[28]. Curtis F. Gerald, *Applied Numerical Analysis,* Second Edition, Addison-Wesley Publishing Company, Reading, MA (1978).

[29]. C. Judson King, *Separation Processes, Second Edition,* McGraw-Hill Book Company, 1980.

[30]. Bernard Tribollet and John Newman, "Analytic Expression of the Warburg Impedance for a Rotating Disk Electrode," *Journal of the Electrochemical Society, 130,* 822-824 (1983).

[31]. Robert V. Homsy and John Newman, "An Asymptotic Solution for the Warburg Impedance of a Rotating Disk Electrode," *Journal of the Electrochemical Society, 121,* 521-523 (1974).

LAWRENCE BERKELEY LABORATORY
TECHNICAL INFORMATION DEPARTMENT
1 CYCLOTRON ROAD
BERKELEY, CALIFORNIA 94720